

Chapter 1

Background Information on Ritterazines and Cephalostatins

1.1 ISOLATION AND BIOLOGICAL DATA

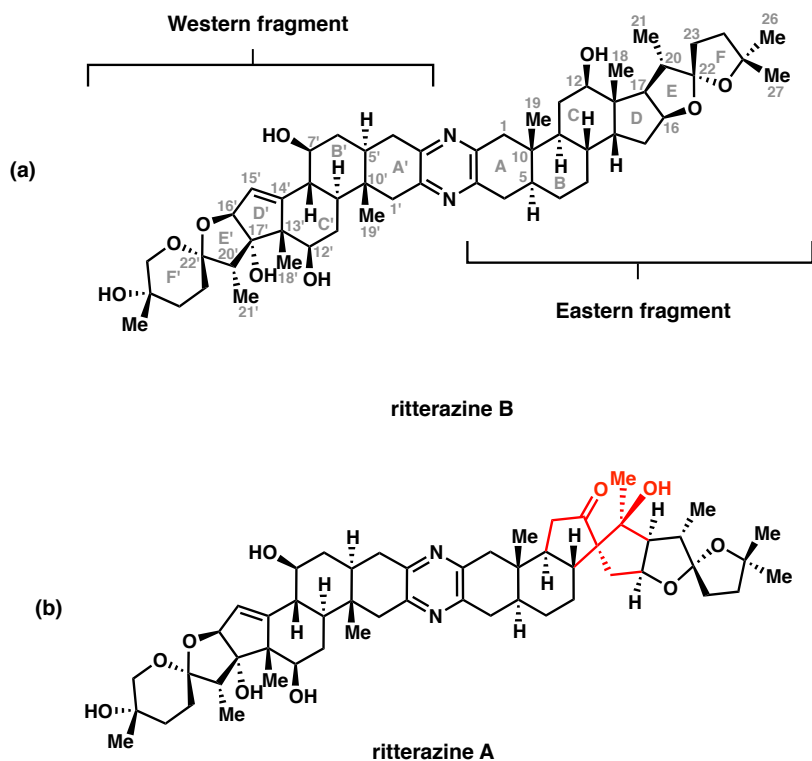
Ritterazines A through Z are natural products that were isolated from the Japanese marine tunicate *Ritterella tokioka* by Fusetani et al, collected at depths of 3–5 m off the Izu Peninsula, 100 km southwest of Tokyo.¹ Tunicates such as *Ritterella tokioka* have found to be a significant source of cytotoxic compounds, including the didemnins, the ecteinascidins, and the patellazoles.¹ Upon isolation via lipophilic extraction, the extracts were found to exhibit potent activity against P388 murine leukemia cells.^{1d} Structurally, ritterazines are dimeric steroidal alkaloids strongly resembling the structures of the cephalostatins.¹ However, the cephalostatins were isolated from the East African hemichordate *Cephalodiscus gilchristi* in the Indian Ocean, hundreds of miles away from the Izu Peninsula.¹ Although these natural products come from different parts of the world, their structure and biological activity is very similar.¹

Ritterazine B (**Figure 1a**) was isolated by Fusetani et al. in 1995, and its structure was found to strongly resemble the previously isolated ritterazine A (**Figure**

¹ a) Fusetani #1 b) Fusetani #2 c) Fusetani #3 d) Fusetani #4

1b).¹ The UV spectrum of ritterazine B contained a peak at λ_{max} 288 nm, which was also found in the spectrum of ritterazine A, indicating that both of these structures include a pyrazine ring.^{1b} This pyrazine ring joins the two steroidal moieties, facilitating deconstruction of the ritterazine structures into the western and eastern fragments. The western half of ritterazine B was determined to possess the same connectivity and stereochemistry as that of ritterazine A. This includes a C14'–C15' unsaturation in the D' ring, hydroxyl groups at C7', C12', and C17', and a 5/6 spiroketal system with the E'/F' rings. The eastern half of ritterazine B is slightly less oxidized, containing a hydroxyl group at C12, and a 5/5 spiroketal.

Figure 1. (a) Structure of western and eastern fragments of ritterazine B with atom labels. (b) Structure of ritterazine A with highlighted differences from ritterazine B.



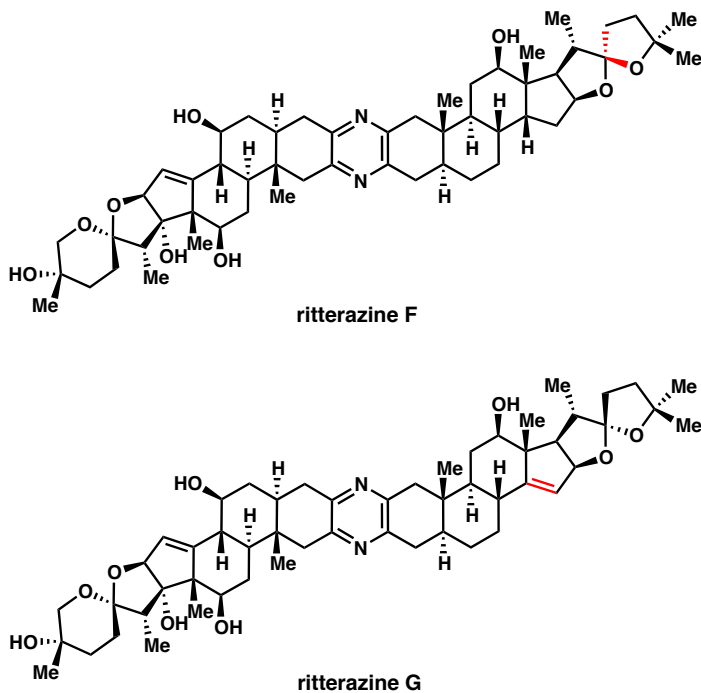
Ritterazine B is the most potent of the ritterazine derivatives isolated to date. Comparison of the various ritterazine structures can provide insight into the structure-activity relationships of ritterazine B that are important for biological activity. **Table 1** shows the cytotoxicity against P388 murine leukemia cells for all ritterazine derivatives. Ritterazines F and G (**Figure 2**) are the two most potent compounds after ritterazine B, and, unsurprisingly, their structures are very similar to ritterazine B. Ritterazine F has the same structure as ritterazine B, except it contains the opposite stereochemistry of the 5/5 spiroketal at C22. Ritterazine G has the same structure as ritterazine B, except that it contains D ring unsaturation.

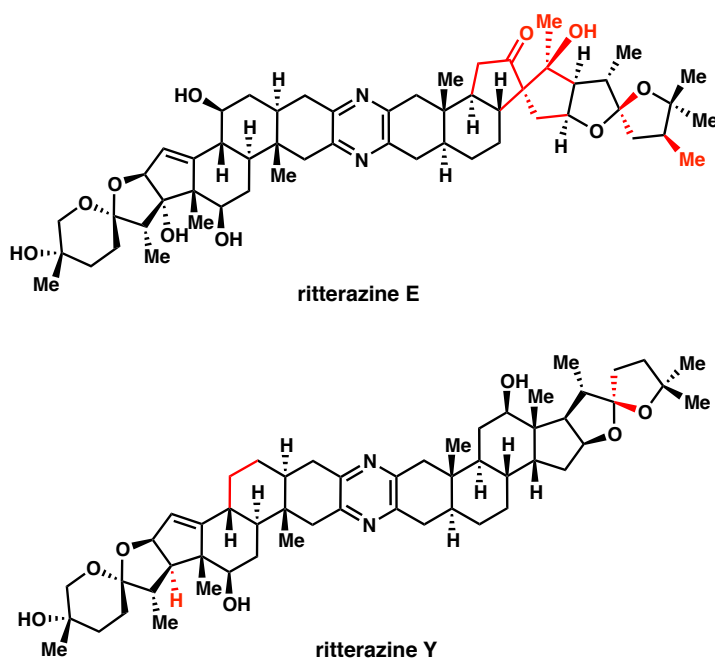
Ritterazines A, E, and Y (**Figures 1c** and **2**, respectively) are also extremely potent compounds. The western fragments of ritterazines A and E are the same as ritterazines B, F, and G, so therefore, the structural components of the western half must be essential for potent biological activity. However, the structures of ritterazines A and E are distinguished by eastern fragments with rearranged steroid skeletons in which the C and D rings are joined as a 5/5 spirocycle. Lastly, ritterazine Y (**Figure 2**) exhibits the same cytotoxicity as ritterazines A and E, however the structure of ritterazine Y lacks the rearranged steroid. The eastern half is the same as ritterazine F, which was shown not to decrease cytotoxicity substantially. However, the decrease in activity from ritterazine F to ritterazine Y comes from the loss of hydroxyl groups at C7' and C17', and therefore indicating that these functional groups increase cytotoxicity.

Table 1. Cytotoxic activity of 26 ritterazine derivatives against P388 murine leukemia cells (IC_{50} , ng/mL).

Ritterazine	IC_{50} (ng/mL)	Ritterazine	IC_{50} (ng/mL)
A	3.5	N	460
B	0.15	O	2100
C	92	P	710
D	16	Q	570
E	3.5	R	2100
F	0.73	S	460
G	0.73	T	460
H	16	U	2100
I	14	V	2100
J	13	W	3200
K	9.5	X	3000
L	10	Y	3.5
M	15	Z	2000

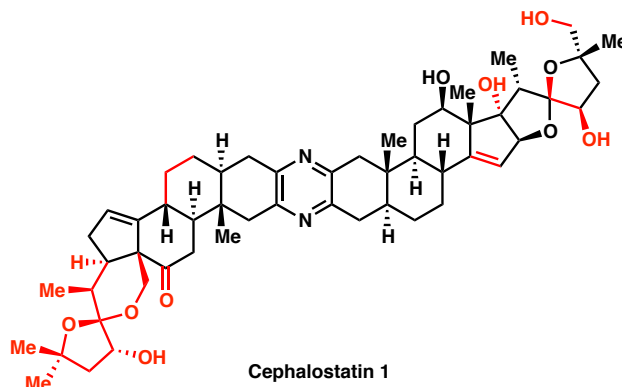
Figure 2. Structures of ritterazines F, G, E, and Y with highlighted differences from ritterazine B.





The related natural product cephalostatin 1 (**Figure 3**) also contains the steroidal dimer joined by a pyrazine ring, however there are some significant structural differences. The eastern half of cephalostatin 1 resembles the eastern fragment of ritterazine B, except that cephalostatin 1 possesses an unsaturated D ring, and the opposite stereochemistry of the 5/5 spiroketal at C22. In addition, cephalostatin 1 is further functionalized with hydroxyl groups at C17, C23, and C27. The western half of cephalostatin 1 differs more significantly from the corresponding ritterazine B fragment. Most strikingly, D' and E' rings are fused at C17' and C13', and the E' and F' rings comprise a 6/5 spirocyclic system.

Figure 3. Structure of cephalostatin 1 with highlighted differences from ritterazine B.



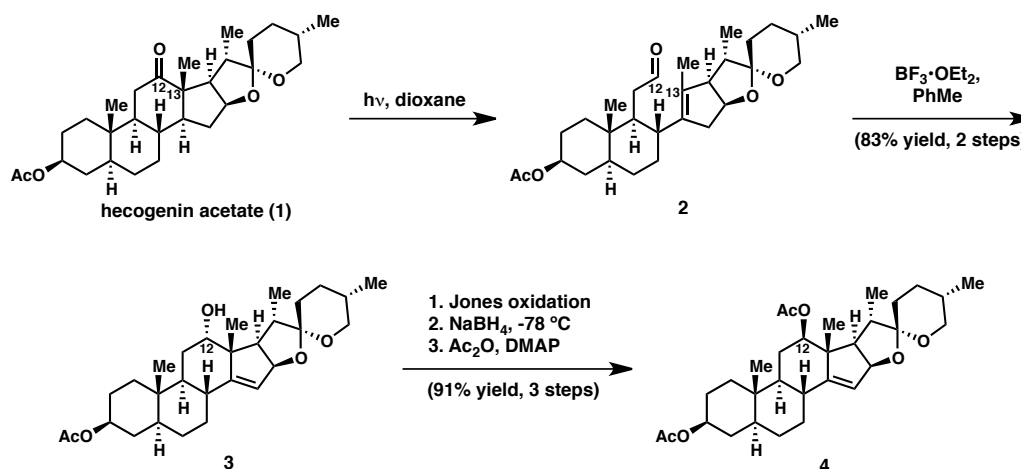
Cephalostatin 1 has more potent biological activity compared to ritterazine B, however analysis of the biological activities indicates that the cellular target and mechanism of action are likely the same. The average GI_{50} values of cephalostatin 1 and ritterazine B against the National Cancer Institute's collection of 60 human cancer cell lines (NCI-60) are 1.8 nM and 3.2 nM, respectively,^{2,3} and the COMPARE correlation coefficient against NCI-10 for cephalostatin 1 and ritterazine B is 0.93, where values greater than 0.60 suggest that the two compounds have a related mechanism of action.^{4,5} Shair et al. has shown that the cellular target of these compounds is oxysterol binding protein (OSBP), and has demonstrated that cephalostatin 1 and ritterazine B change the cellular localization of OSBP to the Golgi, and also cephalostatin 1 (and, most likely, ritterazine B) reduces levels of OSBP to an antiproliferative level.⁵ Shair studied the effects of these natural products on the biosynthesis of sphingomyelin. Ceramide is transported to the Golgi for synthesis of sphingomyelin by ceramide transport protein (CERT), which depends on OSBP and VAP-A.⁵ It was further found that high concentrations of cephalostatin 1

and ritterazine B inhibit the biosynthesis of sphingomyelin.⁵ Although these experiments have produced interesting results, there are still more questions to be answered, and how these natural products bind to OSBP is unknown.

1.2 PRIOR SYNTHETIC STUDIES

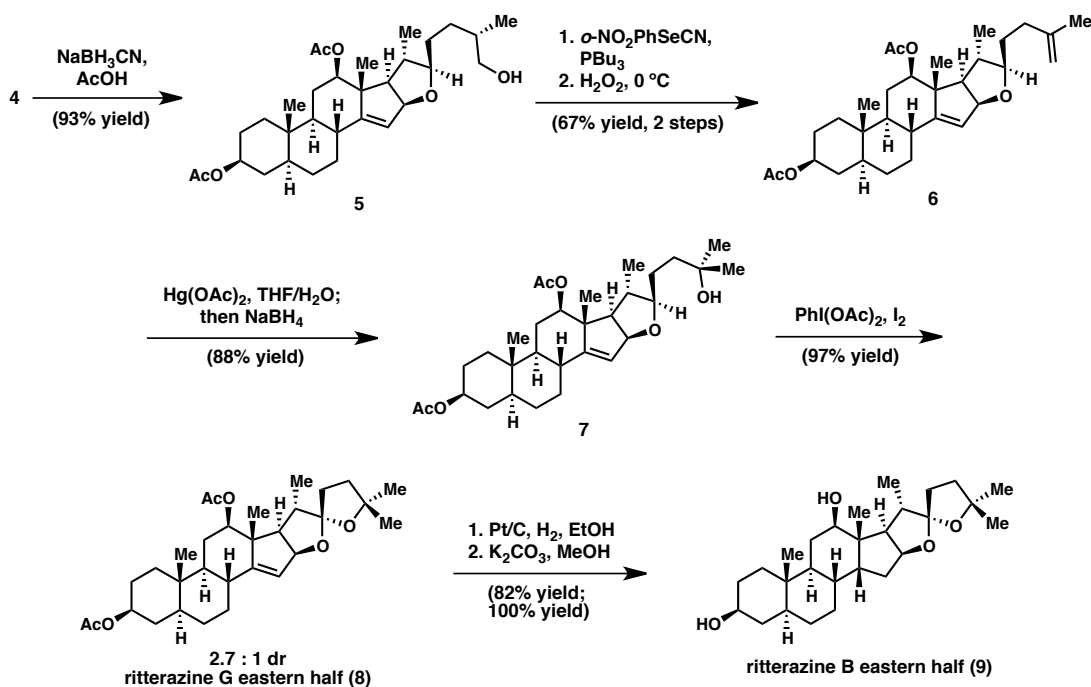
Shair et. al. reported syntheses of the eastern fragments of ritterazines B, F, and G.³ Beginning with the commercially available steroid, hecogenin acetate (**1**), Norrish type I photolytic cleavage of the C12–C13 bond provides aldehyde **2** (**Scheme 1**), which, when treated with $\text{BF}_3 \cdot \text{OEt}_2$, undergoes an ene reaction to reclose the six-membered C ring and produce **3**.³ A three-step procedure involving oxidation to the ketone, diastereoselective reduction to the correctly configured alcohol at C12, and subsequent protection delivers steroid **4**.

Scheme 1. Initial steps in Shair's syntheses of ritterazines B, F, and G eastern halves.



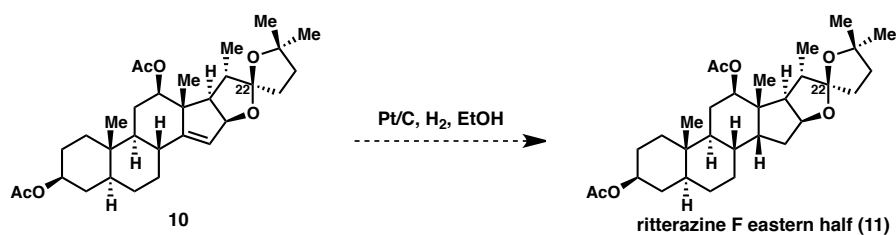
Shair then implements several steps to convert the 5/6 spiroketal of **4** to the desired 5/5 system found in ritterazine G. Reductive opening of the acetal provides primary alcohol **5**, which is subjected to selenation/oxidation following the Grieco protocol to provide alkene **6**. Oxymercuration/demercuration of **6** delivers tertiary alcohol **7**, which is subjected to a Suárez iodine(III)-mediated oxidative ring closure to give the required 5/5 spiroketal. The Suárez reaction produces a 2.5:1 mixture of diastereomers, slightly favoring the desired stereochemistry. After isolating the major diastereomer, Shair uses a two-step procedure to complete the synthesis of the eastern fragment of ritterazine B (**9**). Compound **8** was subjected to hydrogenation with Pt/C in ethanol, and acetyl deprotection to yield the eastern half of ritterazine B (**9**) in 33% overall yield and 11 steps from hecogenin acetate.³

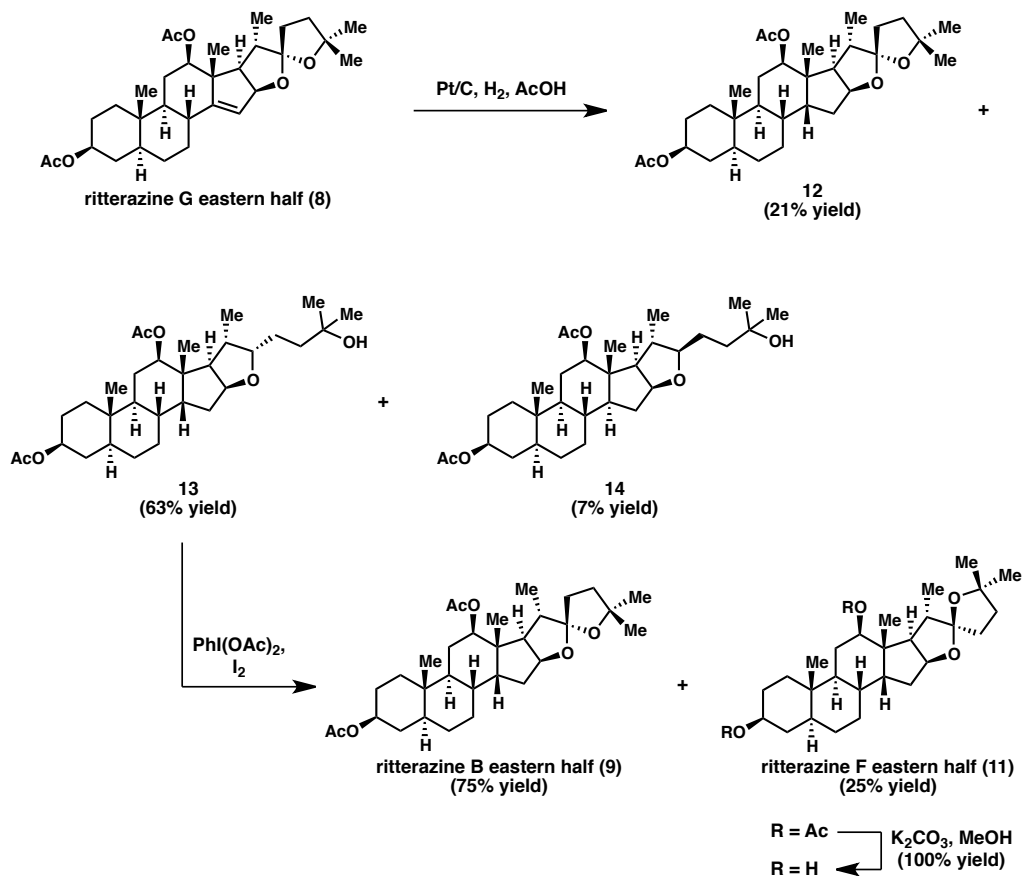
Scheme 2. Completion of Shair's syntheses of ritterazines G and B eastern fragments.



As mentioned previously, the eastern half of ritterazine F has the opposite stereochemistry to ritterazine B at the 5/5 spiroketal, as found in the minor product (**10**) of the Suárez oxidative cyclization. Shair's efforts to reduce the double bond of **10** revealed that the stereochemistry of the spiroketal equilibrates in ethanol, leading to a mixture of products favoring ritterazine G and B (**Scheme 3**).³ This result indicated that the stereochemistry of the 5/5 spiroketal in ritterazines G and B is the thermodynamic configuration.³ In order to form the contra-thermodynamic spiroketal of ritterazine F, Shair hydrogenates compound **8** in acetic acid. This reaction produces a mixture of ketal **12** (21% yield), as well as ring opened diastereomers **13** and **14** (**Scheme 4**). Upon Suárez oxidation of **13**, the desired ritterazine F eastern fragment is produced in 25% yield, due to some equilibration of the ketal to compound **9** under the reaction conditions.

Scheme 3. Shair's attempted hydrogenation to form ritterazine F eastern half.



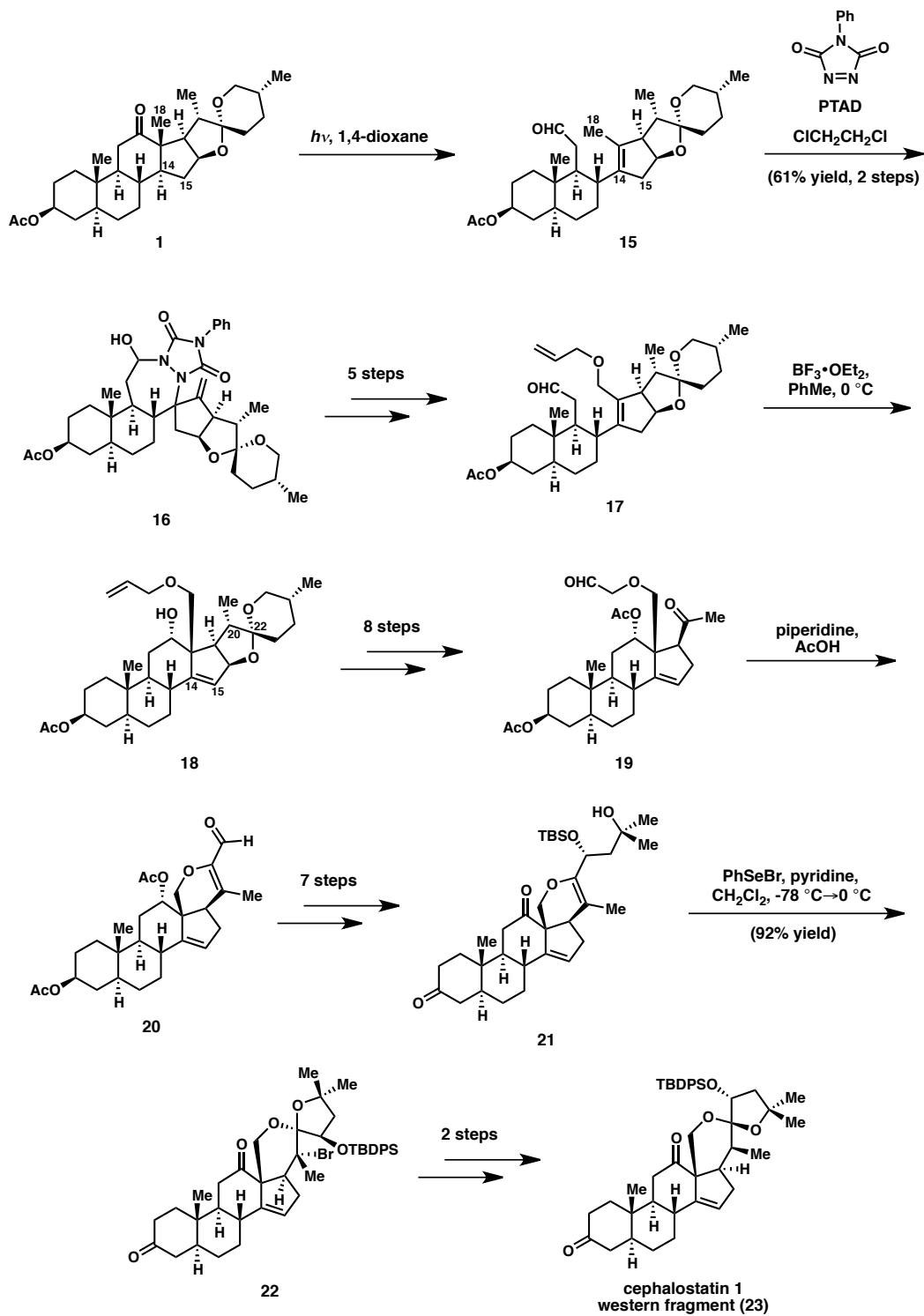
Scheme 4. Shair's endgame for the synthesis of ritterazine F eastern fragment.

Shair has also reported a total synthesis of the related natural product cephalostatin 1.² The synthesis of the western fragment begins from commercially available steroid hecogenin acetate (**1**). The important transformations required to convert this compound to the western fragment of cephalostatin 1 involve installation of the C14–C15 olefin, which is present in the western half of ritterazine B, and rearrangement of the spiroketal. To this end, photolysis of **1** results in type I Norrish reaction to provide aldehyde **15** with a tetra-substituted double bond in the D ring (**Scheme 5**). From here, the synthesis requires selective oxidation of the C18 methyl group and isomerization of the double bond. To achieve these transformations, Shair

employs an unusual allylic oxidation with 4-phenyl-1,2,4-triazoline-3,5-dione (PTAD), which proceeds through an ene reaction to selectively functionalize the C18 methyl group, forming a 7-membered hemiaminal.² Elaboration over five steps delivers aldehyde **17**, which is treated with $\text{BF}_3 \cdot \text{OEt}_2$ to close the C ring and yield compound **18**. This transformation successfully employs the C14–C15 olefin, which is the desired position for cephalostatin 1.

The final major transformation involves rearrangement of the spiroketal. This requires eight steps and involves oxidative scission of the C20–C22 bond to provide ketone **19**. Intramolecular aldol reaction of **19** produces enal **20**, which is homologated to form tertiary alcohol **21**. The spiroketal in the western fragment of cephalostatin 1 was proposed to be in the thermodynamically stable configuration, and it was predicted that treatment of **21** in mild acid would produce the desired spiroketal.² However, this was not the case, and Shair found that the undesired stereoisomer was formed. This was surprising given that the correct stereoisomer was produced by Fuchs et al. in a similar transformation, although Fuchs' substrate lacked the D-ring unsaturation.² In order to resolve this outcome, Shair employed a two-step bromoetherification/reductive debromination sequence. Following bromoetherification of **21** with PhSeBr, compound **22** was subjected to debromination, and then epimerization of the spiroketal with acid to yield the western half of cephalostatin 1.

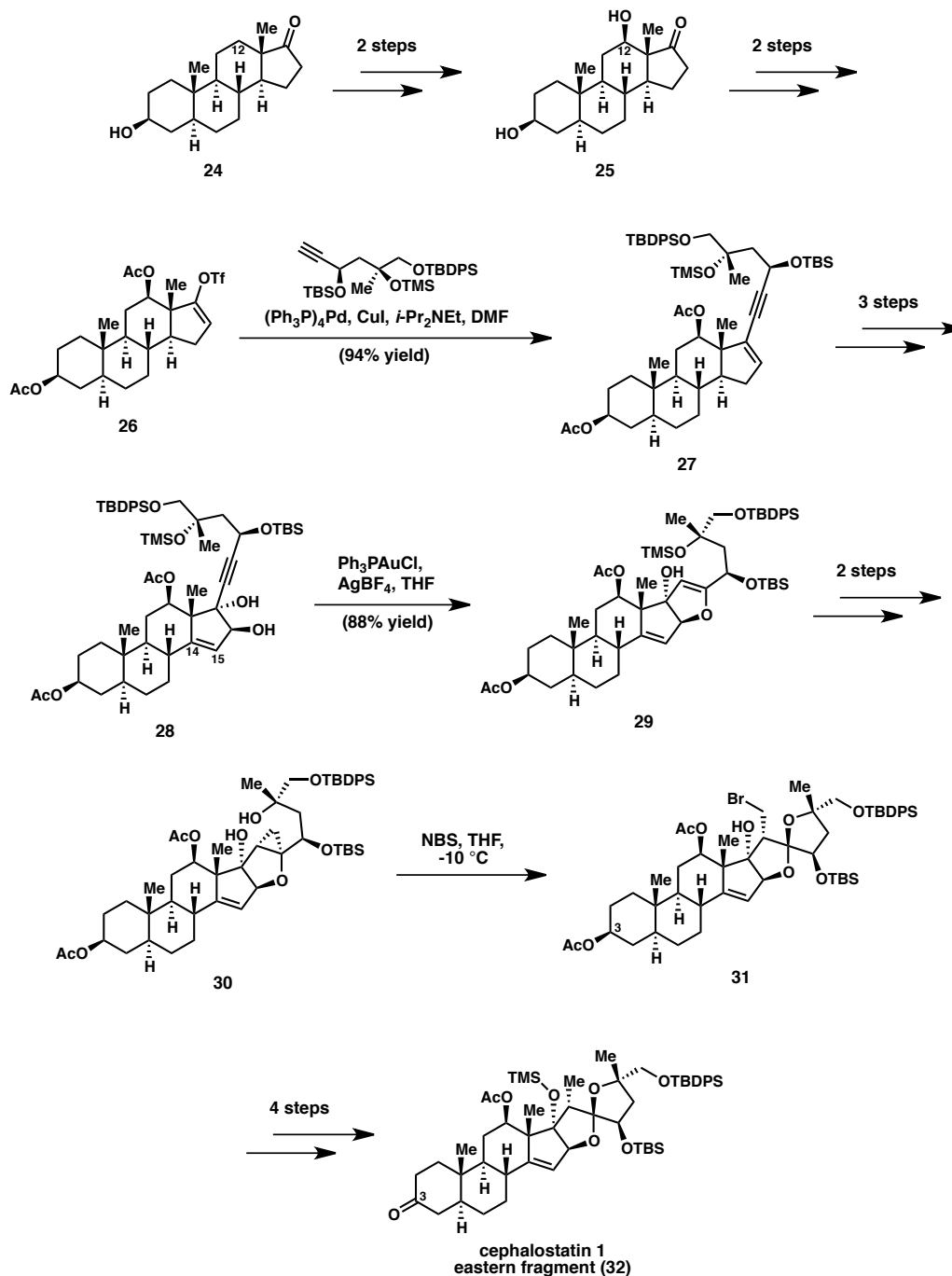
Scheme 5. Shair's synthesis of the western fragment of cephalostatin 1 from commercially available hecogenin acetate.



Shair's synthesis of the eastern fragment of cephalostatin 1 begins with commercially available *trans*-androsterone (**24**). In order to oxidize at C12, Shair employs methodology developed by Shönecker et al. that involves condensation of **24** with 2-(aminomethyl)pyridine in catalytic acid, followed by oxidation with stoichiometric Cu(OTf)₂ in the presence of molecular oxygen to arrive at diol **25**.^{2,7} This second step is rather low yielding (25% yield), and presents the opportunity to develop an improved method for C12 oxidation in the synthesis of ritterazine B. Acetylation of diol **25**, followed by conversion to the corresponding vinyl triflate, provides **26**. This is cross-coupled with a functionalized alkyne fragment using a Pd-catalyzed Sonogashira coupling to produce **27** in 94% yield.

Elaboration of **27** through a three-step sequence provides *trans*-diol **28**, which undergoes a Au(I)-catalyzed 5-endo-dig cyclization to produce **29** in 88% yield. To prepare the precursor for the key spiroketalization, intermediate **29** undergoes Simmons–Smith cyclopropanation, and deprotection of the TMS alcohol to provide **30**. The spiroketal of the eastern half of cephalostatin 1 is the contra-thermodynamic configuration, which required kinetically controlled spiroketalization.² This was achieved under neutral reaction conditions using NBS, which decrease equilibration of the spiroketal to yield **31** as the major diastereomer in a 5:1 separable mixture. Completion of the synthesis of cephalostatin 1 eastern fragment involved debromination, TMS protection of the hindered alcohol, selective deacetylation of the C3 alcohol, and oxidation to the ketone.

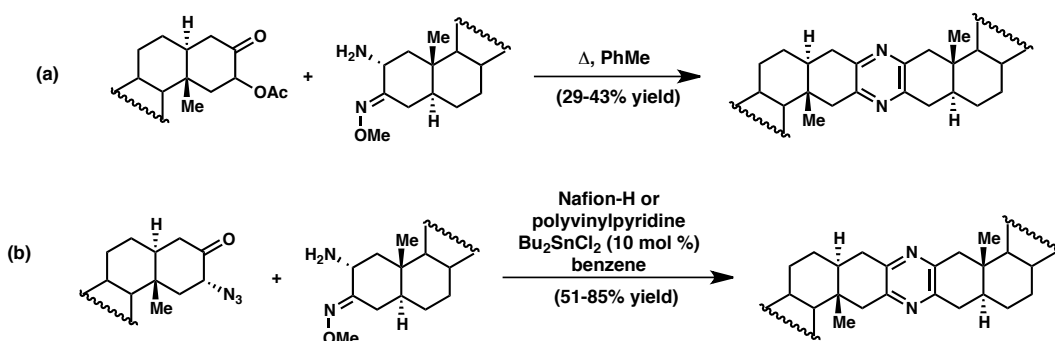
Scheme 6. Shair's synthesis of the eastern fragment of cephalostatin 1 from commercially available *trans*-androsterone.



In order to join the two western and eastern fragments (**23** and **32**, respectively), Shair adapted methodology from Fuchs et al. for unsymmetrical

pyrazine formation.^{8,9} Fuchs' initial studies toward the synthesis of cephalostatin 7 led to the desired unsymmetrical product, as well as homocoupling from each of the coupling partners.⁸ Heathcock et al. had presented a solution to this problem by coupling α -acetoxy ketones with α -amino methoximes (**Scheme 7a**), however the drawback of this methodology is the low yields (29–43% yield).¹⁰ Fuchs et al. subsequently improved upon this protocol by substituting the α -acetoxy ketone with an α -azido ketone (**Scheme 7b**), which greatly improved yields. In Fuchs' synthesis of 14' α ,15'-dihydrocephalostatin 1 analog, he established that the eastern fragment was optimal as the α -amino methoxime, and the western fragment as the α -azido ketone.⁸ Therefore, Shair followed this approach to complete the synthesis of cephalostatin 1.^{2,8}

Scheme 7. (a) Unsymmetrical pyrazine formation by Heathcock et al. (b) Unsymmetrical pyrazine formation by Fuchs et al.



The western fragment of cephalostatin 1 (**23**) was converted to the α -azido ketone **33** through a two-step process. First, α -bromination was achieved with $\text{PhMe}_3\text{NBr}_3$, and the bromide was then converted to the desired azide using tetramethylguanidinium azide and EtNO_2 . The eastern half (**32**) was subjected to the

the same bromination/azidation sequence, which was then followed by formation of the methoxime. Staudinger reduction of the azide moiety to primary amine **33** enabled coupling of intermediates **33** and **34** in the presence of polyvinylpyridine and Bu_2SnCl_2 to produce compound **35**. Completion of the synthesis of cephalostatin 1 was achieved upon global deprotection of the siloxy groups.

Scheme 8. Completion of Shair's total synthesis of cephalostatin 1.

